# Freezing of Subarctic Hillslopes, Wolf Creek Basin, Yukon, Canada

Authors: Carey, Sean K., and Woo, Ming-ko

# Freezing of Subarctic Hillslopes, Wolf Creek Basin, Yukon, Canada

*Sean K. Carey\* and*

*Ming-ko Woo†*

*Department of Geography and
Environmental Studies,
Carleton University, Ottawa, Ontario,
K1S 5B6, Canada.
sean_carey@carleton.ca
†School of Geography and Geology,
McMaster University, Hamilton, Ontario,
L8S 4K1, Canada.

## Abstract

Freezing processes were monitored at five sites within the Wolf Creek basin, Yukon, Canada during the winter of 1998–1999. Ground temperatures were measured using thermocouples in hillslopes that had frost status ranging from permanent to seasonal. The timing of freezing and ground thermal regimes varied among the five sites and was controlled by (1) the variation in surface soil temperature, (2) frost status (seasonal vs. permanent), (3) moisture content of the active layer, (4) properties of the soil profile, and (5) the presence/absence of subsurface drainage. On slopes with permafrost, cooling was rapid and two-sided freezing closed the active layer several months after the onset of freezing. On a slope with seasonal frost only, dry soil conditions allowed frost to penetrate to depth. In contrast, a slope with seasonal frost that had continuous drainage, frost depths were shallow due to heat advected from flowing water. A simple one-dimensional conduction model with latent heat was used to simulate freezing processes. Model performance varied among the slopes, and results indicate that (1) conduction is the predominant heat transfer mechanism during freezing, (2) latent heat is the principal factor controlling frost front descent, and (3) lateral flow significantly retards frost penetration because of heat advection. This information is valuable in assessing spatial variability within tile-based models and in predicting freezing, which defines an effective end-of-season on lateral hydrological processes.

## Introduction

The ability to predict soil freezing is important as it defines an effective end-of-season limit on lateral hydrological processes such as subsurface drainage in permafrost environments and represents a major discontinuity in the hydrological cycle (i.e., the cessation of evapotranspiration). While it is evident that ground thaw in the spring is closely linked to the available energy (Carey and Woo, 1998a), there are few studies that investigate the timing of freezing in the discontinuous permafrost zone (cf. Fox, 1992). Typically, this is due to the practice that hydrologic field investigation often terminates with the cessation of major flow activities. As part of the Canadian GEWEX (Global Energy and Water Cycle Experiment) Enhanced Study (CAGES), data was collected throughout the year to evaluate the winter ground thermal regime.

In the subarctic, there exists considerable variability over short distances in the ground thermal regime, especially within topographically complex areas (Carey and Woo, 2000). Carey and Woo (2001a) quantified the variability in timing and magnitude of hydrologic processes from the onset of thaw until the of end summer, emphasizing the dramatic local-scale variations in water and heat distribution. Like the summer hydrologic studies, the differential timing and depth of freezing among slopes must be compared as they have a strong bearing on winter streamflow. Such information on soil freezing variability, particularly at smaller scales, is important for land-surface hydrological models that seek to integrate hydrological processes over large areas.

Ground thermal and moisture states are closely coupled in frozen soils (Guymon and Luthin, 1974). This coupling becomes increasingly important during the fall freezing period when a large amount of latent heat must be removed. Conduction is widely accepted as the dominant mechanism of heat transfer in soils, although the possibility of convection in frozen soil has been reported in field and laboratory experiments (i.e., Nixon, 1975; Hinkel and Outcalt, 1993, 1994). Two approaches predominate in modelling soil thermal regimes for

permafrost areas: (1) using energy transfer and heat flow theory to formulate detailed one-dimensional heat flow equations, and (2) using empirical models to predict soil temperature from surface meteorological data. In the first approach, the physical and thermal properties of soils are combined with heat flow equations (Romanovsky and Osterkamp, 2000; Roth and Boike, 2001), yet the generality and applicability of these models is restricted by the detailed soil parameters and the small time step required to solve the thermal calculations. Using empirical models that simplify the heat flow equations have found widespread application and often relate soil heat flux to aboveground meteorological conditions, especially air temperature (Ouellet, 1973; Hasfurther and Bunnan, 1974; Bocock et al., 1977; MacLean and Ayres, 1985; Zuzel et al., 1986).

The Stefan formula (Jumikis, 1977) for freezing and thawing in multilayered soil is often used to model seasonal freezing and thawing in the soil profile. This approach avoids the small time steps required by physically based heat flow models and the large data requirements of empirical models. The Stefan equation solves the one-dimensional heat conduction equation while neglecting convective heat flow from precipitation, snow melt, and surface water that although usually negligible (de Vries, 1966), can be an important factor in soil thawing (Kingsbury and Moore, 1987). In addition, the Stefan equation provides an approximate solution to heat conduction under the assumption that sensible heat effects (heat associated with warming the soil profile) are negligible. This is true if latent heat (heat associated with phase change) is much larger than sensible heat or if sensible heat is small; a condition that is true for soils with high water contents (Lunardini, 1981). The Stefan equation is also based on the assumption that soil temperature gradients are linear. When these conditions are met, Stefan's equation provides an accurate approximation of depths of freezing and thawing in soils (Carlson, 1952; Jumikis, 1977; Lunardini, 1981). When they are not met, the equation will yield freezing depths that are too large (Lunardini, 1981) and a correction factor may be applied (Andersland and Ladanyi, 1994).
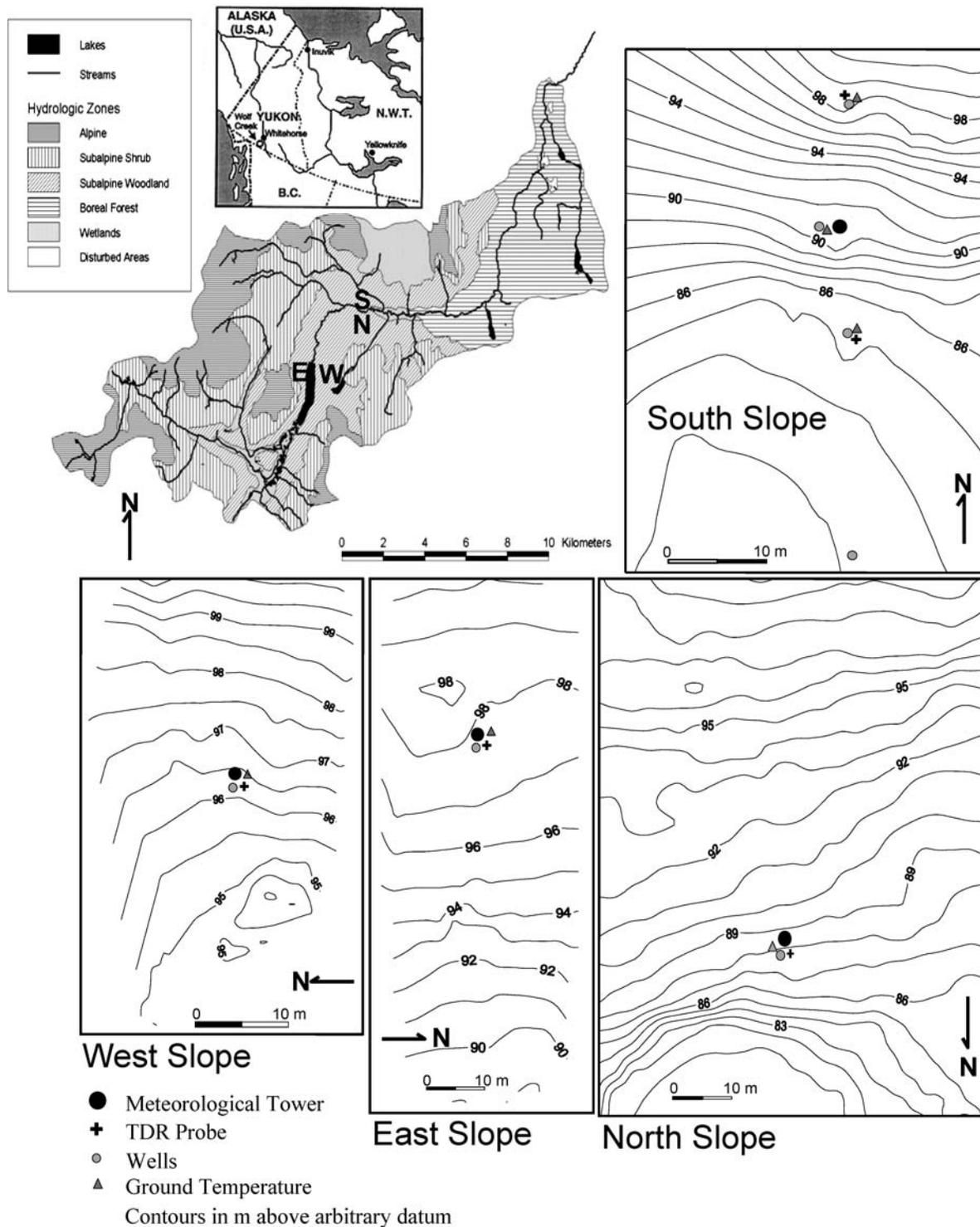
FIGURE 1. *Hydrologic zones and location of experimental slopes within the Wolf Creek Basin, topography of slopes, and location of instrumentation. Inset shows location within Canada.*

Considering that (1) there is little reported data comparing the variability of timing and depth of freezing in mountainous subarctic basins, and (2) simple freezing algorithms are required for macro- and mesoscale hydrological models as complex heat and mass transfer algorithms have little practical importance at larger scales, the objectives of this study are:

(1) to compare the fall freezing conditions of four hillslopes located within a small, subarctic area but with large contrasts in their physical setting, and

(2) to apply a simple one-dimensional ground freezing algorithm based on Stefan's equation to simulate the freezing processes in these slopes.

## Study Site

Four slopes of different orientation were studied within the Wolf Creek Bain (60°31′N, 135°31′W), 15 km south of Whitehorse, Yukon Territory, Canada (Fig. 1). Climatic records from the Whitehorse airport

### TABLE 1

*Physical characteristics of the experimental sites in Wolf Creek basin.*

|  | North slope | South slope | East slope | West slope |
|---|---|---|---|---|
| Elevation (m) | 1175 | 1175 | 1250 | 1250 |
| Slope angle | 18° | 60° | 10° | 17° |
| Vegetation | Open Black/ White spruce | Closed aspen forest | Sparse Black/ White spruce | Willow shrub |
|  | Willow shrub |  | Willow shrub | Labrador Tea |
|  | Labrador Tea |  | Labrador Tea |  |
| Frost | Permafrost (0.8 m) | seasonal frost (1.6 m) | seasonal frost (1.2 m) | permafrost (0.6 m) |

(elevation 703 m) indicate that the study area has a subarctic continental climate characterized by large temperature range and low precipitation. The mean annual January and July temperatures are −21°C and +15°C. Mean annual precipitation is approximately 260 mm, half of which falls as rain (Wahl et al., 1987). Hydrological investigations carried out since 1996 suggests precipitation measured at Whitehorse may underestimate basin precipitation by 25 to 35% (Pomeroy and Granger, 1999).

The experimental slopes are located within a 5-km$^2$ area of the subarctic open woodland ecozone of the basin where permafrost is discontinuous and vegetation consists of black spruce (*Picea mariana*) and white spruce (*Picea glauca*) trees with willow shrubs (*Salix*) and Labrador Tea (*Ledum groenlandicum*) on poorly drained slopes and aspen forests (*Populus tremuloides*) on well drained sites. On some hillslopes, an organic layer overlies less permeable mineral layers, but well-drained slopes have only thin accumulations of leaf litter. The study slopes are labeled according to their principal aspects. The physical setting of each slope is summarized in Table 1. Carey and Woo (2001a) presented detailed site descriptions and water balance information for these hillslopes. The south-facing (S) slope is distinct from the other three slopes in that it has a dense aspen forest without a surface organic layer. The north-facing (N) and west-facing (W) slopes are underlain by permafrost and have similar topography. The N-slope has thinner organic soils, deeper thaw and usually wetter conditions than the W-slope. The east-facing (E) slope has seasonal frost only and an organic layer with a distinct acrotelm-catotelm transition at 0.1 m that separates the periodically aerated, partly living soil layer (acrotelm) and the lower anaerobic layer (catotelm). This slope receives lateral drainage from an upslope alpine area that supplies water to the study site throughout the year to maintain a high water table (Carey and Woo, 2001b).

## Field Methods

Soil parameters (Table 2) were determined by laboratory and field methods outlined in Carey and Woo (2001a). Ground temperatures were measured from 7 September 1998 through the snowmelt period in 1999, using type-T thermocouples referenced to a Campbell CR-10x data-logger with an external resistor as a temperature reference. Using this method, absolute thermocouple accuracy is 0.2 to 0.5°C, however, the relative accuracy between any two sensors was less than 0.05°C allowing for precise gradient calculations. These sensors were installed at various depths between 1995 and 1997 and therefore the disturbed soil had time to adjust to its surroundings. Thermocouple depths were placed at 0.02, 0.05, 0.10, 0.20, 0.40, and 0.60 m at all sites with an additional 1.0 and 1.5 m depth at the S-slope sites and a 0.80 m depth for the E-slope site. Soil water content was measured by Time Domain Reflectometry at the four sites and was calibrated *in situ* (see Table 3 for depths). Campbell Scientific CS-615 water content reflectometer probes buried at the E- and W-slopes allowed continuous monitoring of liquid water content. On the N- and S-slopes, TDR (MoisturePoint) measurements were made when site personnel were available in the summer.

### TABLE 2

*Soil properties of the experimental sites.*

| | North slope | | | Lower south slope | | | Upper south slope | | East slope | | | West slope | | |
|---|---|---|---|---|---|---|---|---|---|---|---|---|---|---|
| | Upper organic (0–0.11 m) | Lower organic (0.11–0.23 m) | Mineral soil (>0.23–0.60 m) | Mineral soil (>0.6 m) | Mineral silt soil (0–0.4 m) | Mineral silt soil (>0.4 m) | Mineral silt soil (0–0.4 m) | Mineral silt soil (>0.4 m) | Upper organic (0–0.1 m) | Lower organic (0.1–0.25 m) | Mineral soil (>0.25 m) | Upper organic (0–0.2 m) | Lower organic (0.2–0.4 m) | Mineral soil (>0.6 m) |
| Bulk density (kg m$^{-3}$) | 55 ± 20 | 90 ± 20 | 1340 ± 180 | 1340 ± 180 | 1420 ± 70 | 1420 ± 70 | 1420 ± 70 | 1420 ± 70 | 74 ± 30 | 130 ± 50 | 1644 ± 120 | 48 ± 20 | 69 ± 20 | 1565 ± 100 |
| Porosity (%) | 92 ± 4 | 84 ± 10 | 52 ± 7 | 52 ± 7 | 55 ± 4 | 55 ± 4 | 55 ± 4 | 55 ± 4 | 86 ± 5 | 77 ± 12 | 4.5 ± 5 | 89 ± 4 | 82 ± 6 | 47 ± 4 |
| Organic fraction | 0.16 | 0.24 | 0.08 | 0.04 | 0.07 | 0.03 | 0.07 | 0.03 | 0.14 | 0.21 | 0.05 | 0.11 | 0.17 | 0.05 |
| Mineral fraction | 0 | 0.04 | 0.45 | 0.49 | 0.45 | 0.45 | 0.45 | 0.45 | 0 | 0.02 | 0.5 | 0 | 0.04 | 0.5 |

TABLE 3

*Input values of volumetric soil water content for the frost model as measured on 1 September 1998. Bold values are estimated.*

| Depth | North slope | Lower south slope | Upper south slope | East slope | West slope |
|---|---|---|---|---|---|
| 0.05 m | 0.26 | 0.12 | 0.16 | **0.55** | **0.40** |
| 0.10 m | 0.31 | 0.15 | 0.17 | 0.75 | 0.47 |
| 0.20 m | 0.56 | 0.18 | 0.18 | 0.77 | **0.47** |
| 0.40 m | 0.46 | 0.23 | 0.22 | **0.45** | 0.21 |
| 0.60 m | 0.47 | 0.26 | 0.24 | 0.52 | 0.22 |
| 1.00 m | — | 0.24 | 0.15 | **0.47** | — |

There was no compensation of soil moisture sensors for changes in ionic concentration during freezing.

# Model for Freezing

A one dimensional heat conduction model with phase change was used to calculate ground freezing. A similar model, based upon Stefan's equation (Jumikis, 1977), was employed by Fox (1992) to simulate freeze-thaw depths in permafrost and seasonal frost terrain. For soil freezing, it is assumed that latent heat is the principal heat source to be overcome before the descending coldness causes a downward propagation of the frost front.

The approximate boundary condition at the moving interface separating the frozen and thawed phase is

$$\lambda\theta\frac{dz_f}{dt} = F_+ - F_- \tag{1}$$

where $dz_f/dt$ is the rate of freezing front descent, $\lambda$ is the latent heat of fusion (J m$^{-3}$), $\theta$ is the volume fraction of the soil water content, and $F_+$ are $F_-$ are the heat fluxes (W m$^{-2}$) in the frozen and unfrozen phase, respectively.

Stefan's formula assumes a material to be initially at the isothermal condition at the freezing point, $T_f$, whose surface temperature is lowered to a freezing value $T_s < T_f$. Neglecting heat flow from the underlying thawed material, the boundary condition at the freezing point (eq. 1) becomes

$$\lambda\theta\frac{dz_f}{dt} = F_+ = -k_f\frac{\partial T}{\partial z_f} \tag{2}$$

where $k_f$ is the thermal conductivity of the frozen soil (J m$^{-1}$ s$^{-1}$ K$^{-1}$). If the temperature profile in the frozen zone is assumed to be linear, equation (2) becomes

$$\lambda\theta\frac{dz_f}{dt} = -k_f\frac{T_s - T_f}{z_f} \tag{3}$$

or

$$\Delta z_f = \left[\frac{2k_f(T_s - T_f)}{\lambda\theta}\right]^{1/2} \tag{4}$$

To estimate $k_f$, we use the equation provided by Johansen (1975, quoted in Farouki 1981):

$$k_f = (k_{sat} - k_{dry})(\theta/\phi) + k_{dry} \tag{5}$$

with $\phi$ being the soil porosity. The saturated thermal conductivity ($k_{sat}$) is calculated following Farouki (1981)

$$k_{sat} = \prod_{n=1}^{5} k(j)^{f(j)} \tag{6}$$

with $k(j)$ and $f(j)$ being the thermal conductivity and volumetric fraction of the $j$th type of substance making up the soil (including mineral and organic materials, ice, water, and air, so that there are five types of substance in a soil), and the thermal conductivity for dry soil ($k_{dry}$) (Farouki 1981) is

$$k_{dry} = \frac{(0.135\rho_b + 64.7)}{(2700 - 0.947\rho_b)} \tag{7}$$

where $\rho_b$ is the soil bulk density. For saturated soil, the fractional air content is assumed to be zero. It is further assumed that there is a minimum fractional water content that would not freeze under subfreezing conditions and for the environment of the study area, $f_{min}(water)$ is set to 0.1, based on time-domain reflectometry measurements in the winter.

The ground surface temperature converted to freezing degree-days ($D$), defined as the absolute difference between the 0.02 m average daily temperature and 0°C, drives the model, with the daily average freezing degree-days expressed in degree/second. The computational procedure follows the formulation in Jumikis (1977):

(1) The soil column is divided into $n$ slabs of $\Delta Z$ thickness, each with its specified physical properties including bulk density ($\rho_b$), porosity ($\phi$), mineral and organic contents ($f_m$ and $f_o$), and minimum unfrozen moisture content ($\theta_{min}$) as a lower limit for the volumetric water content $\theta$.

(2) The soil water content of each slab before the freezing season is interpolated from field measurements, to enable the calculation of the $k_f$ values for all the slabs.

(3) The thermal resistance of various slabs is calculated to represent the resistance to the transmission of the freezing temperature down the soil column.

$$R = z_f/k_f \tag{8}$$

where $z_f$ and $k_f$ are the thickness and the thermal conductivity of the frozen soil above the frost front. The parameter $R$ has units of m$^2$ s K J$^{-1}$.

(4) When the frost front reaches slab $m$, the number of degree days needed to freeze the slab ($N$) is

$$N(m) = \lambda\theta\Delta x\left[\sum_{j=1}^{m-1} R(j) + R(m)/2\right] \tag{9}$$

where $0 < \Delta x < \Delta Z$ is the thickness of the unfrozen zone within slab $m$.

(5) If the degree-days available ($D$) exceeds the degree-days required to freeze the slab, (i.e. $D > N$), slab $m$ will be frozen, and the frost will proceed to slab $m + 1$, while the remaining degree-days available to freeze the lower slab is $(D - N)$ through repeating step 4, until the residual degree-days are exhausted.

(6) If the degree-days available is less than the coldness to be overcome (i.e., $D < N$), only partial freezing of the slab occurs and the freezing depth within layer $m$ is calculated by

$$\Delta z_f = -k_f(m)\sum_{j=1}^{m-1} R(j)$$
$$+ \left\{k_f(m)^2\left[\sum_{j=1}^{m-1} R(j)\right]^2 + [2k_f(m)N(m)/\lambda\theta]\right\}^{1/2} \tag{10}$$

and $\Delta z_f$ is converted to daily frost table descent. The parameter $\Delta z_f$ is added to $\sum\Delta Z$ for the $m - 1$ slabs to get the depth of the new frost front. The unfrozen thickness of slab $m$ becomes $\Delta x = \Delta Z_m - \Delta z_f$.

(7) The steps are repeated until the freeze up period is concluded.
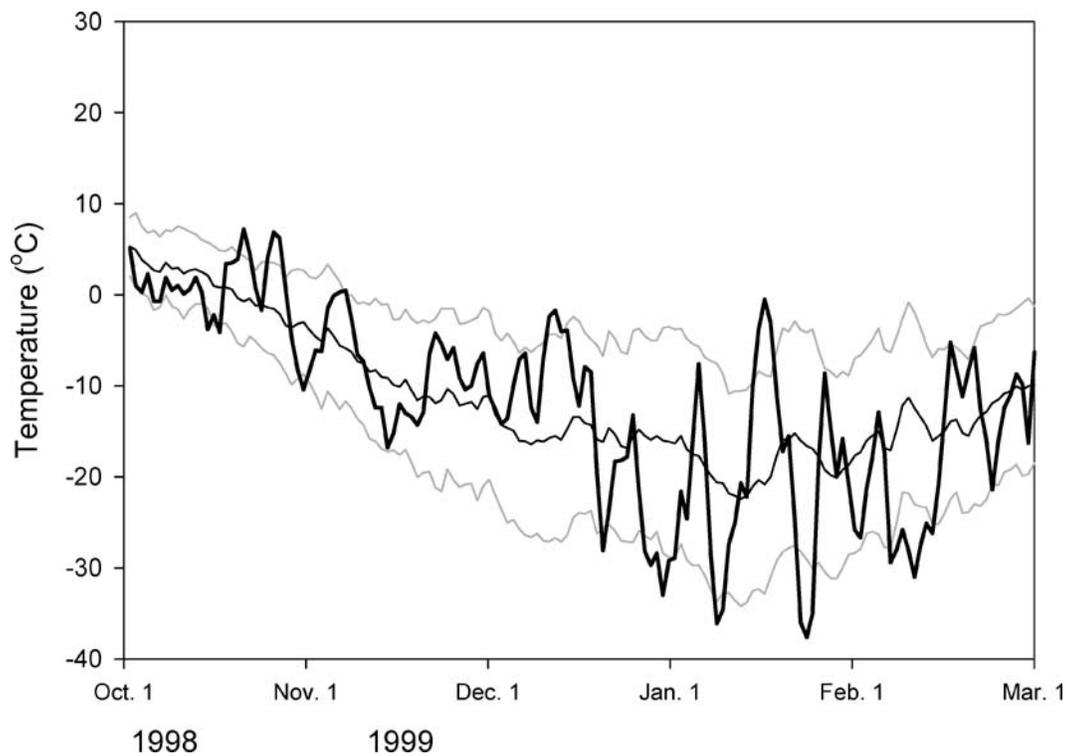
FIGURE 2. *Average daily air temperature of CAGES winter (1998–1999) at Whitehorse (heavy line), compared with long-term mean (thin line)* ± *standard deviation (gray line) values.*

# Results

## CLIMATIC CONDITIONS

Precipitation at the Whitehorse airport indicate that the CAGES study year was slightly drier than the 30-yr normal. However, temperatures were approximately normal, yet exhibited large deviation about the mean (Fig. 2). For the fall freezing period, mean daily temperatures fell below 0°C on 28 October and remained at or below freezing until the onset of melt in the following year.

Soil temperature at 0.02 m depth was used as input to the model. Plots of the daily temperatures at this depth for the experimental sites are shown in Figure 3. The N-slope appeared to have acquired its stable winter snow cover by late September so that the 0.02 m temperature remained at the freezing point even when air temperature fluctuated around 0°C. The snow cover was not fully established at other sites until late October as there were occasions when their 0.02 m temperature rose above 0°C. Even then, the W-slope snow cover insulated the soil poorly as it did not dampen the daily fluctuations of the 0.02 m temperatures. While the E-slope was the warmest during most parts of the winter, the S-slope was particularly cold between December and February.

## GROUND FREEZING REGIME

After the air temperature dipped below 0°C, each study plot acquired a distinct freezing pattern. On the W-slope, the descent of the freezing front began on September 29, about 1 mo ahead of other slopes that commenced their freezing around 26 October (Fig. 4). The low temperature episodes of early November, notably colder for the W-slope than the other slopes, probably accelerated the freezing front descent. Later, a two-sided freezing was observed as the 0°C isotherm appeared at the 0.6 m level on 22 October and rose to intersect the descending freezing front on 22 November, thus completing the freezing of the entire soil column.

After 1 October, the near-surface ground temperature of N-slope remained around 0°C until 26 October, and the active layer became isothermal during this period (Fig. 5). Previous research (Carey and Woo, 1998a) indicated that this isothermal period is the time when discharge from the hillslope base causes significant icing formation. The descent of the 0°C isotherm was initially rapid within the organic layer, reaching 0.25 m in the first 4 d. The rate of freezing declined and generally occurred linearly between 0.25 and 0.6 m on 22 December. Although thermocouples were installed only down to 0.6 m, ground probing on 5 September indicated a maximum active layer depth of 0.8 m. Projection of the 0°C isotherm and neglecting upward freezing indicates that complete freezing of the active layer would have likely occurred around 5 January. Compared with the W-slope, a thicker active layer and the delayed initiation of freezing in the N-slope led to a longer freezing period. After the N-slope freezing, lateral drainage that caused icing formation at the hillslope base effectively ceased until the following spring melt period.

The S-slope had neither permafrost nor a covering layer of organic soil. The two sites within this slope had low but different soil water content contents (Fig. 6). Starting from 26 October, the 0°C isotherm began to descend concurrently in both sites. The rate of frost front descent was greater at the lower site with slightly drier conditions than the upper site. The maximum frost depth for both sites was attained in late February, reaching 1.18 m at the upper slope and 1.5 m at the lower site. The low moisture content, the lack of an insulating porous organic surface layer and the coldest near-surface ground temperatures among the several sites probably contributed to the attainment of the deep freezing in the S-slope. Additionally, a reduced snowpack accumulation on the S-slope due to increased canopy interception and sublimation (Carey and Woo, 2001a) allows colder atmospheric temperatures to reach the ground.

The persistence of a near-surface water table within the E-slope sustained by continuous lateral subsurface flow acted to limit ground freezing. Soil cooling began after snow fell on 28 September but the descent of the 0°C isotherm commenced on 26 October (Fig. 7). The

S. K. CAREY AND M.-K. WOO / 5
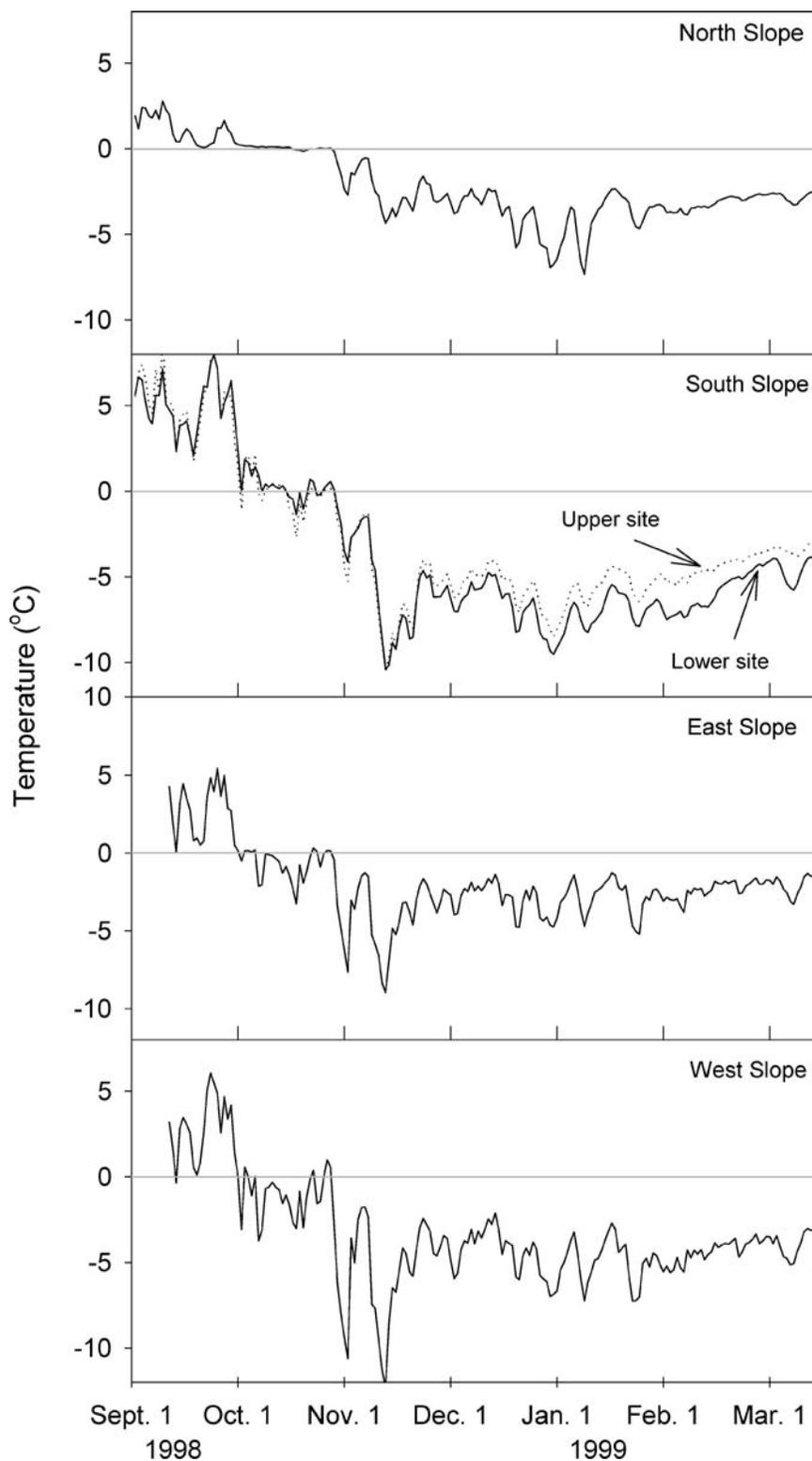
FIGURE 3. Daily mean ground temperature at 0.02 m depth, Wolf Creek experimental sites.

freezing front proceeded rapidly through the top 0.18 m of unsaturated organic materials. As this front moved into the saturated portions of the organic and mineral substrate, the rate of soil freezing declined. Saturated conditions and heat advection by the continuous lateral flow of water at depth prevented ground frost from penetrating deeper than 0.55 m.

### MODELED FREEZING

The model was applied to the four slopes for the winter of 1998–99 using the soil parameters and initial soil water content conditions shown in Table 3. The initial soil water contents were estimated from profile measurements (Table 3, extrapolated beyond the lowest depth of measurement) that were made several days before freezing, assuming moisture drainage in the interim for the N- and S-slopes which did not have continuous monitoring of soil moisture. Ground temperature measured at 0.02 m provided the degree-day inputs to drive the model. Using such data instead of air temperature avoids the inaccuracy of having to estimate the ground surface temperature under a snow cover.

The modeled freezing is compared to measured ground temper-
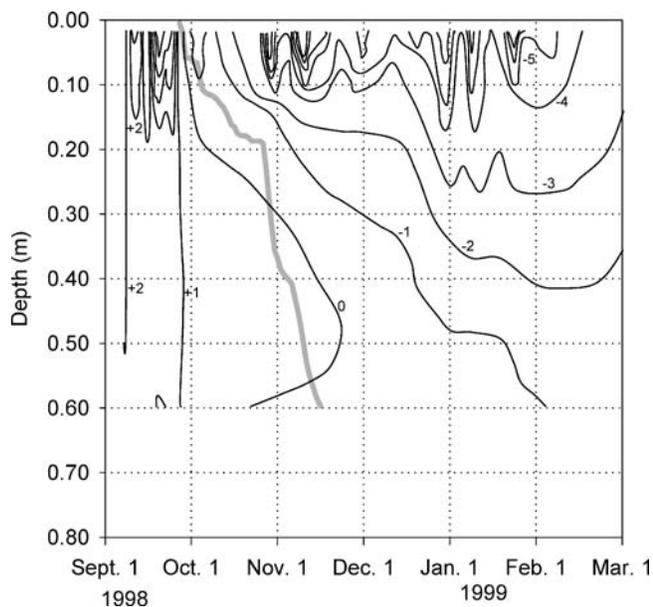
FIGURE 4. Observed ground temperature interpolated from measurements at depths of 0.02, 0.05, 0.10, 0.20, 0.40, and 0.60 m (solid lines) and modeled freezing front (shaded line) for West-slope site. Temperatures are in degrees Celsius.



FIGURE 5. Observed ground temperature interpolated from measurements at depths of 0.02, 0.05, 0.10, 0.20, 0.40, and 0.60 m (solid lines) and modeled freezing front (shaded line) for North-slope site. Temperatures are in degrees Celsius.

atures in Figures 4 to 7. For the lower S-slope site (Fig. 6), the measured and modeled freezing agree closely until 0.9 m is reached, whereupon the modeled depth continues to advance while the observed 0°C isotherm descent becomes more gradual. For the upper S-slope, modeled frost closely approximates the measured 0°C isotherm for several days, and then it diverges and closely follows the +1°C isotherm down to 1.5 m depth.

For the N-slope (Fig. 5), the observed descent of the 0°C isotherm is initially greater than the modeled freezing within the upper 0.25 m of the soil profile, after which the descent of the frost-front becomes more gradual so that the modeled and observed 0°C isotherms gradually converge. At about 0.6 m depth, the measured and modeled frost depths coincide, and based on a maximum active layer thickness of 0.8 m, the modeled active-layer closure occurs by 6 January.

Modeled freezing of the W-slope (Fig. 4) proceeds slower than the observed freezing rate within the top 0.2 m which, like the N-slope, froze within a few days of the initiation of frost. After the freezing of the organic layer, the modeled descent of the frost-front is more rapid than the observed value but the actual completion of active layer freezing was accelerated by upward freezing from the permafrost table.

The E-slope (Fig. 7) shows an initial correspondence in the descent of the observed and modeled freezing fronts down to 0.2 m. Then, the modeled 0°C isotherm descends faster than the observed values. The overestimation of frost-depth gradually increases with time as the model drives the 0°C isotherm downwards while the actual freezing-front descent becomes negligible by 30 January. This divergence is attributed to the continued saturation and heat advection maintained by lateral inflow to the slope (Carey and Woo, 2001b) that are not incorporated in the simulation model.

*MODEL SENSITIVITY*

Based on assumed errors, parameters were varied in isolation on a homogenous soil to evaluate how these changes affect soil freezing. The model was sensitive to changes in the 0.02 m driving temperature that is used to calculate degree-day. The difference between maximum and minimum freezing depth based a total difference of 0.5°C (the maximum measurement error) was approximately 7%. Model sensitiv-

ity to soil moisture changes was similar; an absolute difference of 20% in volumetric moisture content accounted for an 8% difference in freezing depth. Adjusting the minimum unfrozen water content by 5% had a less than 1% influence on freezing depth, indicating that errors in estimation of this parameter have only a small effect on simulated freezing. Altering the volumetric constituents of the soil based on assumed measurement error (5%) influenced freezing by less than 2%. From the sensitivity tests, it is evident that the greatest source of model error based on measurement uncertainty will be generated from imprecise 0.02-m temperature measurement and soil moisture values throughout the profile.
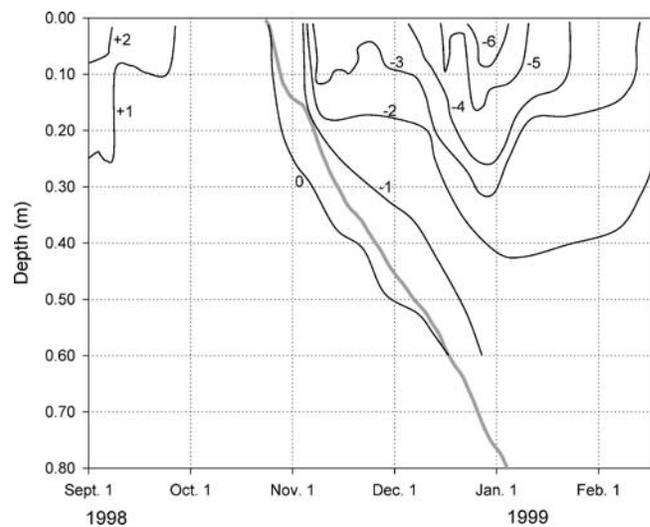
## Discussion

Within a 5 $km^2$ area of a subarctic, subalpine catchment, ground temperatures exhibit large variability in their freezing regime. The establishment of an enduring snowpack by late October is an annual occurrence, placing an upper temperature limit of 0°C at the soil surface but insulating the ground from extreme air temperatures that often fall below −30°C.

Although both N- and W-slopes are underlain by permafrost, their freezing rates were found to be different. Frost descended the W-slope rapidly during October 1998 while an isothermal condition was sustained in the active layer of the N-slope. This latter phenomenon was in part due to the persistent 0°C condition at the ground surface of the N-slope and saturated conditions that sustained an isothermal profile, a feature typical of permafrost environments (Williams and Smith, 1989). However, despite this zero-curtain effect (when the temperature of the active layer remains nearly constant at 0°C ), Romanovsky and Osterkamp (2000) suggest that there are no inherent difficulties in using heat conduction modeling when there is a lack of significant temperature gradients. During this period, subsurface drainage has been previously observed (Carey and Woo, 1998a), which also acts in delaying freezing by advecting heat and contributing to icing formation at the hillslope base.

The role of lateral subsurface flow on inhibiting freezing is further illustrated by the E-slope where throughflow occurs throughout the winter period. The penetration of frost was limited to just over 0.5 m, despite climatic and physical characteristics of soil similar to those of the permafrost-underlain W-slope. The effect of subsurface drainage in preventing the formation of permafrost or in developing a deep active

S. K. Carey and M.-K. Woo / 7
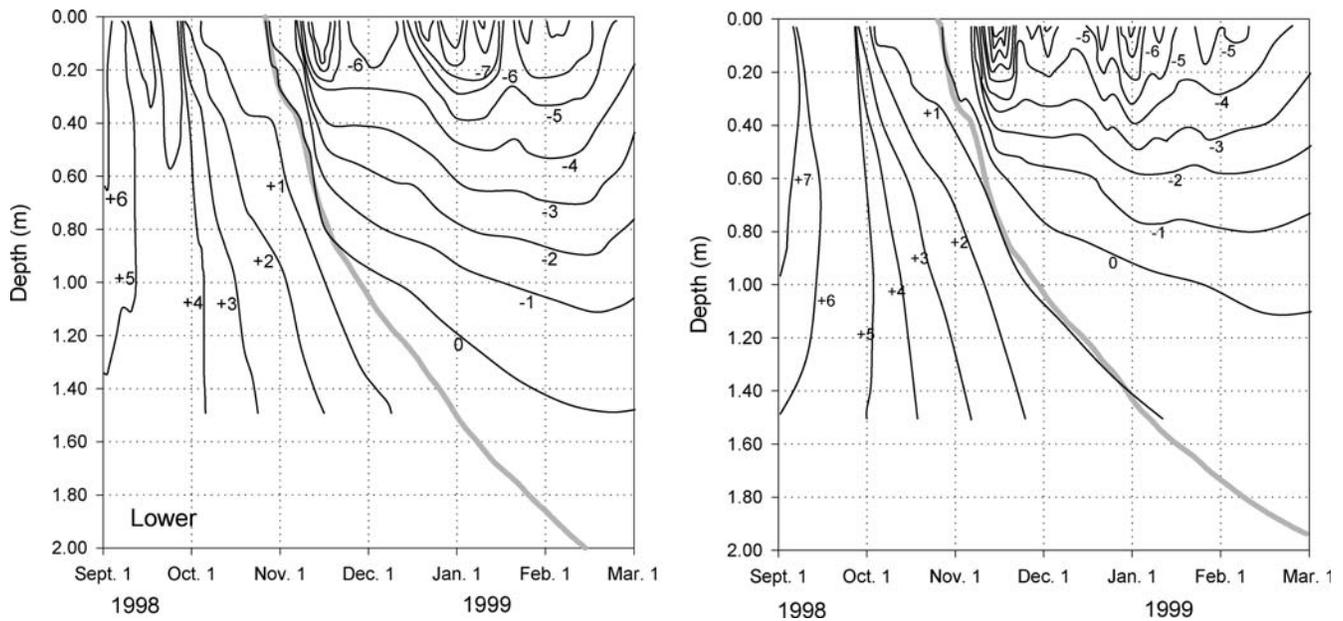
FIGURE 6. *Observed ground temperature interpolated from measurements at depths of 0.02, 0.05, 0.10, 0.20, 0.40, 0.60, 1.00, and 1.50 m (solid lines) and modeled freezing front (shaded line) for South-slope sites. Temperatures are in degrees Celsius.*

layer has been previously noted in other subarctic slopes (Dingman, 1971; Carey and Woo, 2000).

Unlike the other sites with an organic mat atop the mineral substrate, the S-slope has a thick and homogenous silt column that facilitates vertical hydrologic exchanges, with rain and snow meltwater dissipated principally by evapotranspiration and some deep percolation (Carey and Woo, 2001a). At no time was a water table observed within the top 2 m of the soil profile. Although drier conditions at the lower hillslope site may seem counter-intuitive, the lack of lateral moisture redistribution and the greater exposure at this site encourage drier conditions and permits deeper frost penetration. At both sites, maximum freezing was reached in late February, which is later than all other slopes.
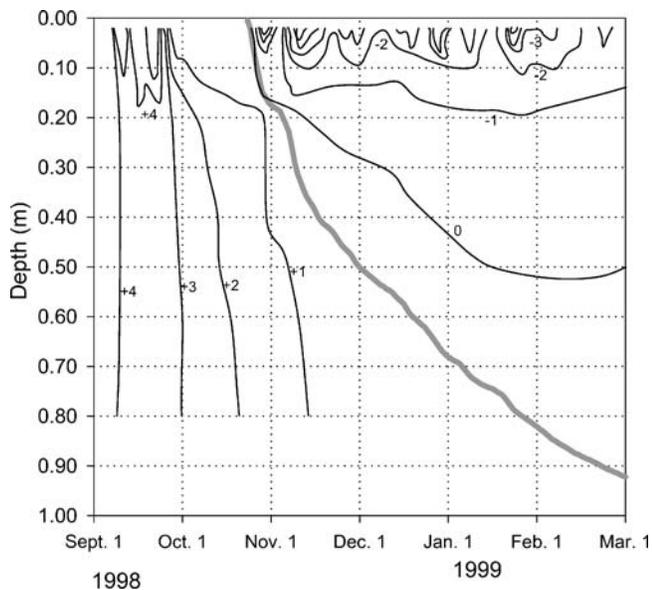


FIGURE 7. *Observed ground temperature (interpolated from measurements at depths of 0.02, 0.05, 0.10, 0.20, 0.40, 0.60, and 0.80 m) and modeled freezing front (shaded line) for East-slope site. Temperatures are in degrees Celsius.*

In spite of the generalized soil profile, the Stefan equation based model was able to reproduce the salient features of slope freeze-back and simulate the key spatial contrasts in slope freezing patterns. While there are many more sophisticated models of heat and mass transfer in permafrost soils, the advantage of using a simple Stefan based model is that it can be applied broadly in a spatial context with fewer input parameters and a larger time-step.

Discrepancies between measured and modeled frost front advance are due to the combined effect of measurement and parameter estimation errors and the absence of a process that significantly affects soil freezing. There are several possible sources of model error:

(1) The model appears most sensitive to the driving surface temperature. Considering that absolute thermocouple accuracy is 0.2 to 0.5°C, this will have a significant influence on calculations of frost-table descent.
(2) The value of initial soil water content for the columns is important considering latent heat is the primary mechanism that controls the descent of the frost front. Extrapolation of moisture conditions beyond the lowest depth of measurement will also cause inaccuracies.
(3) There is no consideration of the migration of moisture to the freezing front (Guymon and Luthin, 1974), possibly leading to an underestimation of the duration of the zero curtain and mismatch with the observed results.
(4) Convection and advection of heat are not considered. While convection is usually considered negligible in soil freezing (Nixon, 1974), advection of heat from lateral drainage (e.g., subsurface inflow or seepage in support of icing formation) occurs on certain slopes, retarding freezing and causing a considerable error in model estimates.
(5) For heat conduction, the Stefan equation assumes a linear temperature profile within the frozen soil, though under a snow cover, fluctuation of sub-freezing temperature is unlikely to be large.
(6) No heat flux from under the freezing front is considered. This may be an important source of heat for nonpermafrost sites, particularly during late winter and spring.
(7) The model considers only unidirectional downward freezing

8 / ARCTIC, ANTARCTIC, AND ALPINE RESEARCH

of the soil, while it is well known that two-sided freezing occurs in permafrost areas (Mackay, 1983), a situation that occurs in the W- and N-facing slopes. However, the rate of up-freezing from the permafrost is usually small relative to the down-freezing rate.

Modeling provides insight into the freezing processes operating in the subarctic slopes. Given that the model only simulates conduction as the mechanism of heat transfer, agreement between modeled and measured results implies that heat conduction processes predominate in the freezing period. Latent heat is employed in the model as the principal factor that controls the frost front descent which makes soil moisture a governing factor in the rate and the depth of freezing. It also follows that lateral inflow and continued saturation of the soil significantly retards frost penetration, as is demonstrated by the E-slope where the modeled freezing differs from the observed values because lateral advection of heat associated with drainage on hillslopes is not included in the model. Other mechanisms of heat dissipation not considered in the model, such as cooling of the soil column, are likely to be much less significant (as has been verified by field studies in permafrost environments, see Carey and Woo [1998b]).

There has been little field evidence of the large variability in ground freezing in subarctic catchments, where slope, aspect and topographic position have a significant impact on hydrological processes (Carey and Woo, 2001a). Documenting this variability, and evaluating the principal factors that cause it is of significant scientific importance considering a primary objective of the Canadian GEWEX program to improve cold-region process representation in large-scale hydrological and land-surface models. Current soil freezing routines are rudimentary and often developed for temperate environments (Verseghy, 1991; Soulis et al., 2000). In cold regions, it is vital to evaluate the key processes controlling freezing variability as the transition from the thawed to the frozen state is a critical discontinuity in the northern hydrological cycle. While the model presented in this study is simple compared with detailed complex heat and mass transfer models, it does provide a means to evaluate the dominant heat transfer mechanisms in the zone of discontinuous permafrost. Additionally, simple algorithms retain their usefulness in macro-scale hydrological models, where parameterization over large areas and longer computational time steps are required (Smirnova et al., 2000; Soulis et al., 2000).

## Conclusions

Slopes that are located close to each other in a topographically complex area can exhibit large variations in the timing, rate and depth of ground freezing. During the CAGES year, freezing of the experimental sites began after a snow cover was established on the slopes. The descent of the frost front was retarded where high soil moisture content was encountered in the soil profile and where heat was laterally advected to a site via subsurface throughflow. The S-slope, with low moisture content and the absence of an insulating organic layer was subject to the fastest and the deepest freezing. In contrast, the east slope fed by lateral inflow had a shallow freezing. Slopes underlain by permafrost, including the N- and W-slopes, experienced two-sided freezing where up-freezing from the permafrost table occurred simultaneously with downward freezing from the cold surface.

Modeling allows corroboration of the major freezing processes not observed in the field, and assesses the roles of various freeze-back mechanisms reported in the literature but not evaluated in terms of their relative magnitudes. In spite of the simplicity of the one-dimension frost model and the need to interpolate and extrapolate soil conditions for model parameterization and initialization, there was some success in simulating the descent of the frost front. Differences between the modeled freezing with the observed 0°C isotherm suggest that while

conduction is the principal mechanisms of heat transfer and latent heat controls thaw, there are other heat mechanisms present such as advective heat transfer associated with lateral subsurface drainage that influence freezing in subarctic slopes.

## References Cited

Andersland, O. B., and Ladanyi, B., 1994: *An Introduction to Frozen Ground Engineering*. New York: Chapman and Hall. 352 pp.

Bocock, K. L., Jeffers, J. N. R., Lindley, D. K., Adamson J. K., and Gill, C. A., 1977: Estimating woodland soil temperature from air temperature and other climatic variables. *Agricultural Meteorology,* 18: 351–372.

Carey, S. K. and Woo, M.-K., 1998a: Snowmelt hydrology of two subarctic slopes, southern Yukon, Canada. *Nordic Hydrolology,* 29: 331–346.

Carey, S. K. and Woo, M.-K., 1998b: The role of ground ice in active layer thaw. *Proceedings, Seventh International Conference on Permafrost,* Yellowknife, Northwest Territories, Canada, Centre d'études nordiques, Université Laval, 127–131.

Carey, S. K. and Woo, M.-K., 2000: Within slope variability of ground heat flux, Subarctic Yukon. *Physical Geography,* 21: 407–417.

Carey, S. K. and Woo, M.-K., 2001a: Spatial variability of hillslope water balance, Wolf Creek basin, subarctic Yukon. *Hydrological Processes,* 15: 3113–3132.

Carey, S. K. and Woo, M.-K., 2001b: Slope runoff processes and flow generation in a subarctic, subalpine environment. *Journal of Hydrology,* 253: 110–129.

Carlson, H., 1952: Calculation of depth of thaw in frozen ground. *Frost Action in Soils: A Symposium.* United States National Research Council, Highway Research Board, 192– 223.

de Vries, D. A., 1966: Thermal properties of soils. *In* Van Wijk, W. R. (ed.), *Physics of Plant Environment.* 2d ed. Amsterdam: North-Holland, 210–235.

Dingman, S. L. 1971: Hydrology of the Glen Creek Watershed, Tanana Basin, Central Alaska. *U.S. Army CRREL Research Report,* 297. 110 pp.

Farouki, O. T., 1981: Thermal properties of soils. U.S. Army *CRREL Monograph,* 81-1. 136 pp.

Fox, J. D., 1992: Incorporating freeze-thaw calculations into a water balance model. *Water Resources Research,* 28: 2229–2243.

Guymon, G. L. and Luthin, J. N., 1974: A coupled heat and moisture transport model for arctic soils. *Water Resources Research,* 10: 995–1001.

Hasfurther, V. R. and Burman, R. D., 1974: Soil temperature modeling using air temperature as a driving mechanism. *Transactions of the American Society of Agricultural Engineers,* 17: 78–81.

Hinkel, K. M. and Outcalt, S. I., 1993: Detection of nonconductive heat transport in soils using spectral analysis. *Water Resources Research,* 29: 1017–1023.

Hinkel, K. M. and Outcalt, S. I., 1994: Identification of heat-transfer processes during soil cooling, freezing and thaw in Central Alaska. *Permafrost and Periglacial Processes,* 5: 217–235.

Jumikis, A. R., 1977: *Thermal Geotechnics.* New Brunswick, N.J.: Rutgers University Press. 375 pp.

Johansen, O., 1975: Thermal conductivity of soils. PhD thesis, University of Trondheim, Norway. 312 pp.

Kingsbury, C. M. and Moore, T. R., 1987: The freeze-thaw cycle of a subarctic fen, northern Quebec, Canada. *Arctic and Alpine Research,* 19: 289–295.

Lunardini, V. J., 1981: *Heat Transfer in Cold Climates.* New York: Van Nostrand Reinhold. 731 pp.

Mackay, J. R., 1983: Downward water movement into frozen ground, western arctic coast, Canada. *Canadian Journal of Earth Sciences,* 20: 120–134.

MacLean, S. F. and Ayres, M. P., 1985: Estimation of soil temperature from climatic variables at Barrow, Alaska, U.S.A. *Arctic and Alpine Research,* 17: 425–432.

Nixon, J. F., 1975: The role of convective heat transport in the thawing of frozen soils. *Canadian Geotechnical Journal,* 12: 425–429.

Ouellet, C. E., 1973: Macroclimatic model for estimating monthly soil temperatures under short-grass cover in Canada. *Canadian Journal of Soil Science,* 53: 263–274.

Pomeroy, J. W. and Granger, R. J., 1999: *Wolf Creek Research Basin: Hydrology, Ecology, Environment.* Environment Canada. 160 pp.

Romanovsky, V. E. and Osterkamp, T. E., 2000: Effects of unfrozen water on heat and mass transport in the active layer and permafrost. *Permafrost and Periglacial Processes,* 11: 219–239.

Roth, K. and Boike, J., 2001: Quantifying the thermal dynamics of a permafrost site near Ny-Alesund, Svalbard. *Water Resources Research,* 37: 2901–2914.

Smirnova T. G., Brown, J. M., Benjamin, S. G., and Kim, D., 2000: Parameterization of cold-season processes in the MAPS land-surface scheme. *Journal of Geophysical Research,* 105: 4077–4086.

Soulis, E. D., Snelgrove, K. R., Kouwen, N., Seglenieks, F., and Verseghy, D. L., 2000: Towards closing the vertical water balance in Canadian atmospheric models: coupling of the Land Surface Scheme CLASS with the distributed hydrological model WATFLOOD. *Atmosphere-Ocean,* 38: 251–269.

Verseghy, D. L., 1991: CLASS – A Canadian Land Surface Scheme for GCMs, I. Soil Model. *International Journal of Climatology,* 11: 111–133.

Wahl, H. E., Fraser, D. B., Harvey, R. C., and Culp, E. H., 1987: *Climate of the Yukon.* Environment Canada, Atmosphere Environment Service. Climatological Studies No. 40, Ottawa. 87 pp.

Williams, P. J. and Smith, M. W., 1989: *The Frozen Earth: Fundamentals of Geocryology.* Cambridge: Cambridge University Press. 306 pp.

Zuzel, I. F., Pikul J. L., and Greenwalt, R. N., 1986: Point probability distributions of frozen soil. *Journal of Climate and Applied Meteorology,* 25: 1681–1686.

*Revised ms submitted October 2004*